JOURNAL OF MATERIALS SCIENCE 27 (1992) 2406–2412

Microstructure and microcracking behaviour of barium zirconium phosphate ($BaZr_4P_6O_{24}$) ceramics

D. A. REGA, D. K. AGRAWAL, C.-Y. HUANG, H. A. McKINSTRY
Materials Research Laboratory, Pennsylvania State University, University Park, PA 16802, USA

Barium zirconium phosphate ($BaZr_4P_6O_{24}$), a member of a new family of low-thermal-expansion materials known as NZP, was synthesized by the solution sol–gel method, and sintered ceramics were prepared at 1100–1600 °C. The effect of sintering parameters such as time and temperature on the microstructure and phase composition was studied. $BaZr_4P_6O_{24}$ is known to possess anisotropy in its axial thermal expansions, which usually causes microcracking in the sintered bodies when cooled. The microcracking activity of the sintered samples was examined by acoustic emission measurements.

1. Introduction

Barium zirconium phosphate ($BaZr_4P_6O_{24}$, BaZP) belongs to a large family of new low-expansion materials known as NZP after $NaZr_2P_3O_{12}$ which is a prototype composition [1, 2]. NZP has recently attracted wide interest [3–7] for its potential applications as an optical mirror substrate in space telescopes; fast ionic conductors; catalyst supports; hosts for immobilizing radioactive waste; and ceramic components in the automobile industry. NZP's crystal structure allows numerous ionic substitutions at various lattice sites, leading to new compositions as well as controlling the physical properties [8]. The basic crystal structure of NZP is rhombohedral and consists of a three-dimensional network of strongly bonded PO_4 tetrahedra and ZrO_6 octahedra linked by corner sharing to form a stable but flexible framework [9]. The Na or Ba, or any other substituent ion, is located in the interstitial sites or in the structural holes created by the framework. Many NZP materials demonstrate not only low overall thermal expansion behaviour but an anisotropy in their lattice thermal expansion [5, 10–12]. Thermal expansion anisotropy usually leads to microcracking when a material is cooled from the sintering temperature.

For a non-cubic material to be of practical use in anti-thermal shock applications, it must not only have an overall low thermal expansion, but it must also have a low anisotropy in its lattice thermal expansion. In a ceramic body when grains expand (and/or contract) differently in different directions due to a thermal gradient, regions of uneven stress develop within the body. When the stress exceeds the internal strength of the ceramic body, microcracking occurs [13]. In ceramics, microcracking is usually observed when the grain size exceeds a critical value below which no microcracks form [14]. This critical grain size is inversely proportional to the square of the difference in the axial thermal expansions, $\Delta\alpha$. The microcracks can greatly affect the mechanical properties and the overall thermal expansion behaviour of the material.

In the past it has been difficult to study and observe the formation of microcracks due to the lack of a sensitive technique [15, 16]. Electron microscopic techniques have been used extensively to observe cracks (large and small) in sintered ceramic bodies. However, very small (in size and number) microcracks, as in the case of BaZP and similar low anisotropic materials, are difficult to observe by scanning or transmission electron microscope. Thermosonimetry or acoustic emission is a technique which measures sonic emissions that transport energy through mechanical waves [16], and can be used to study phenomena involving microdeformations such as phase changes, kinetics of crystallization of glasses, movement of dislocations, and thermal microcracking.

$BaZr_4P_6O_{24}$ has been reported to have a bulk linear coefficient of thermal expansion of $3.37 \times 10^{-6}\,°C^{-1}$ and axial thermal expansions of 5.4×10^{-6} and $-1.8 \times 10^{-6}\,°C^{-1}$ (between 25 and 500 °C) along the a and c axes, respectively [12]. In the present study, the effect of sintering parameters such as time and temperature on the microstructure and phase composition of the sintered samples of BaZP was investigated. Further, acoustic emission measurements were carried out on selected samples in order to determine the microcracking activity of the sintered bodies.

2. Experimental procedure

2.1. Powder preparation and sample fabrication

$BaZr_4P_6O_{24}$ was synthesized using a solution sol–gel method as described by Lenain *et al.* [17]. Stoichiometric amounts of aqueous solutions of $Ba(NO_3)_2$ and $ZrOCl_2 \cdot 8H_2O$ were mixed first, and then the appropriate amount of $NH_4H_2PO_4$ solution was added to

0022–2461

the mixture drop by drop with continuous stirring to achieve homogeneous mixing. As the phosphate solution was added, a viscous gel was formed, which was dried for 2 days at 90 °C and then hand-ground into a fine powder. This powder was calcined for 24 h at 600 °C to remove Cl_2, NH_3 and nitric oxides. The calcined material was ground with a mortar and pestle to −325 mesh, and pressed under 200 MPa into sample discs (20-mm in diameter) using polyvinyl alcohol (PVA) as a binder.

The samples were sintered for various times at various temperatures. At 1100, 1200 and 1300 °C, the samples were sintered for 0.2, 0.5, 1, 2, 5 and 10 h at each temperature, and at 1600 °C for 0.25 and 1 h. Before final heat treatment, all the samples were first heated at 500 °C for 4 h to burn out the binder.

2.2. Characterization

The sintered specimens were characterized for their density by determining the geometrical dimensions and weight; for phase composition by using powder X-ray diffractometry (XRD; Scintag Scientific Computer and Instruments Co.); for microstructure using scanning electron microscopy (SEM; International Scientific Instruments Co.); and for microcracking activity by the acoustic emission technique. In the acoustic emission method described elsewhere [15], samples sintered at 1300 and 1600 °C were measured only since they showed near phase pure material. A specimen bar of approximately 3 × 5 × 15 mm was attached to one end of an alumina rod (acts as waveguide) with high-temperature cement. The other end of the rod was coupled to a transducer with a water-soluble ultrasonic couplant. The transducer is capable of detecting signals in the range of 300–700 kHz with median frequency of 500 kHz. The sample was heated in the furnace to 700 °C and then cooled at a rate of 10 °C min^{-1}. The acoustic signals were detected and recorded only during the cooling cycle, and no activity was observed during the heating cycle.

3. Results and discussion

3.1. Density measurements

The average geometrical green density of BaZP specimens was calculated to be 2.08 g cm^{-3}. The theoretical density was determined to be 3.44 g cm^{-3} using the lattice parameters a and c for a hexagonal system as given in the JCPDS file (34-95) for $BaZr_4P_6O_{24}$. The density data for the sintered BaZP ceramics are presented in Fig. 1. In general, the sintered densities are low, the maximum density achieved was about 2.54 g cm^{-3} (74% of theoretical) at 1600 °C for 1 h. A

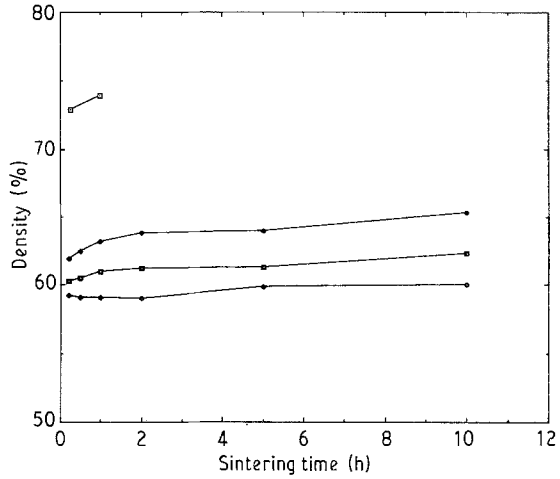

Figure 1 Sintered densities of BaZP samples as a function of sintering time and temperature. ⊡, 1600; ◆, 1300; ■, 1200; ◇, 1100 °C.

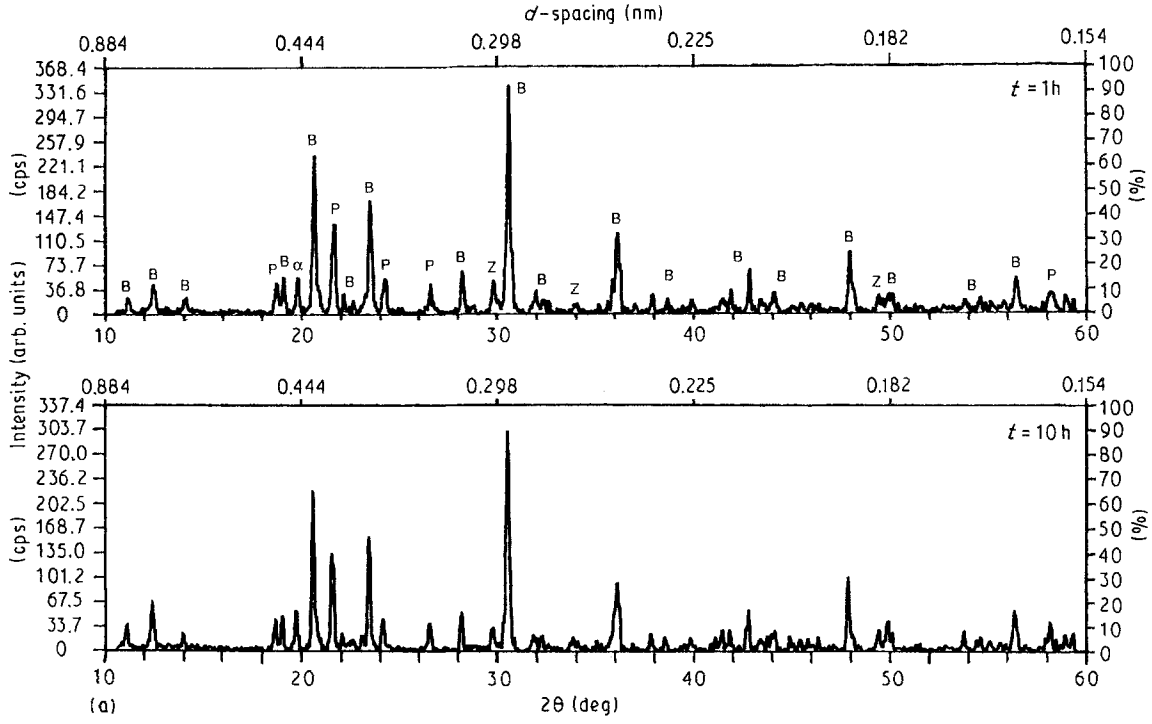

Figure 2 XRD patterns of BaZP samples sintered at (a) 1100, (b) 1200 and (c) 1300 °C, showing BaZP (B) as the major phase and ZrO_2 (Z), ZrP_2O_7 (P) and α-$BaZr(PO_4)_2$ (α) as minor phases.

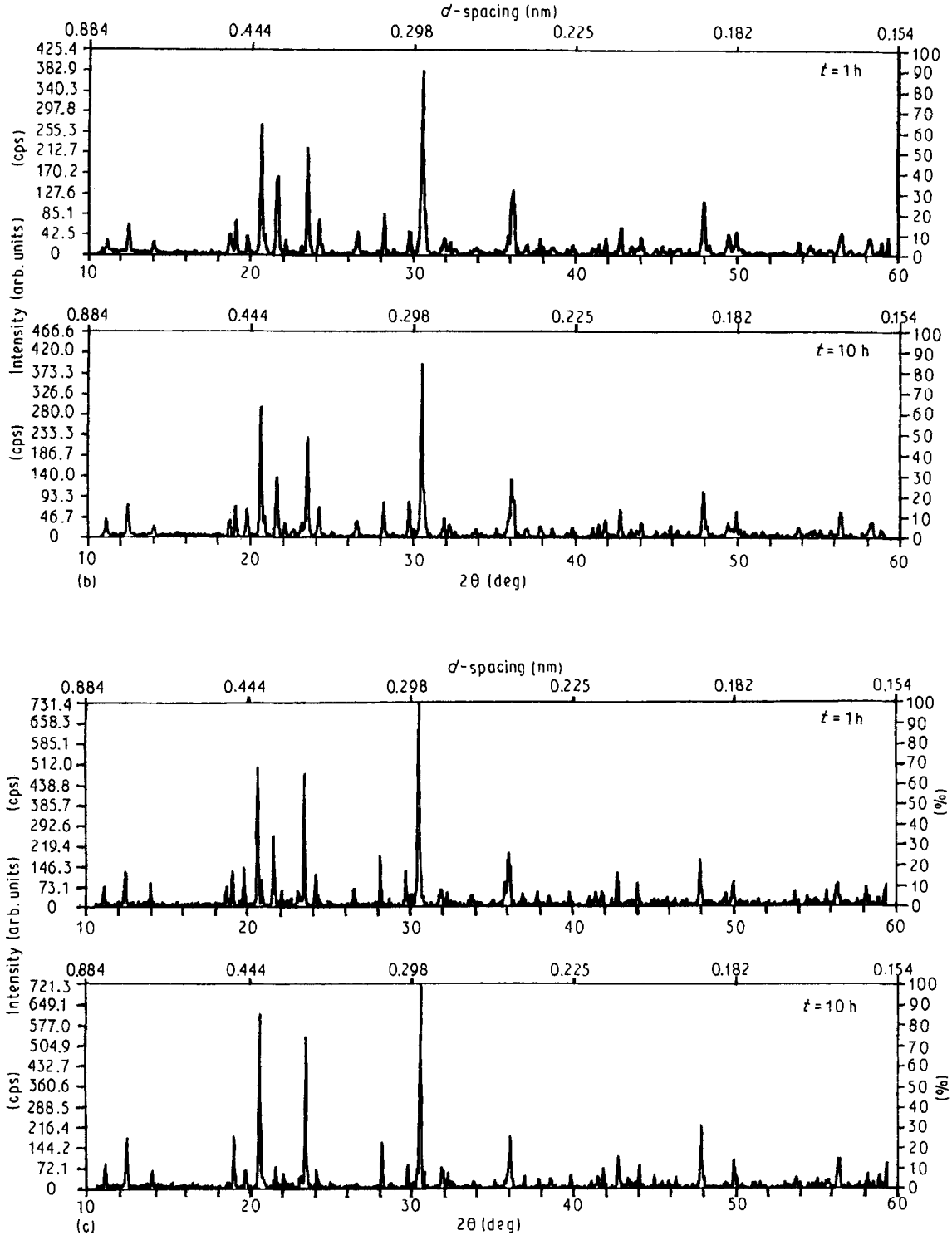

Figure 2 Continued

general trend can be observed that the density increased with the sintering time and temperature. It is believed that if longer sintering times are employed, the density of BaZP ceramics can be enhanced substantially.

3.2. Phase identification

The calcined BaZP powder was found to be X-ray amorphous, evidenced by the absence of any diffraction peaks in its XRD pattern. The XRD patterns of the samples sintered at 1100, 1200 and 1300 °C for 1 and 10 h are shown in Fig. 2, and at 1600 °C for 0.25 and 1 h in Fig. 3. For the 1100 °C samples, the major phase was $BaZr_4P_6O_{24}$ and zirconium pyrophosphate (ZrP_2O_7), ZrO_2 and α-$BaZr(PO_4)_2$ were present as minor crystalline phases, which decreased with increasing sintering time. A similar trend was observed in the samples sintered at 1200 and 1300 °C except the amounts of minor phases had decreased further, indicating that the reaction of the formation of $BaZr_4P_6O_{24}$ had not yet been completed and may require higher temperature and/or longer sintering time. The XRD pattern of the sample sintered at 1600 °C (Fig. 3) for 1 h shows nearly single-phase material, and the sample sintered for 0.25 h shows very

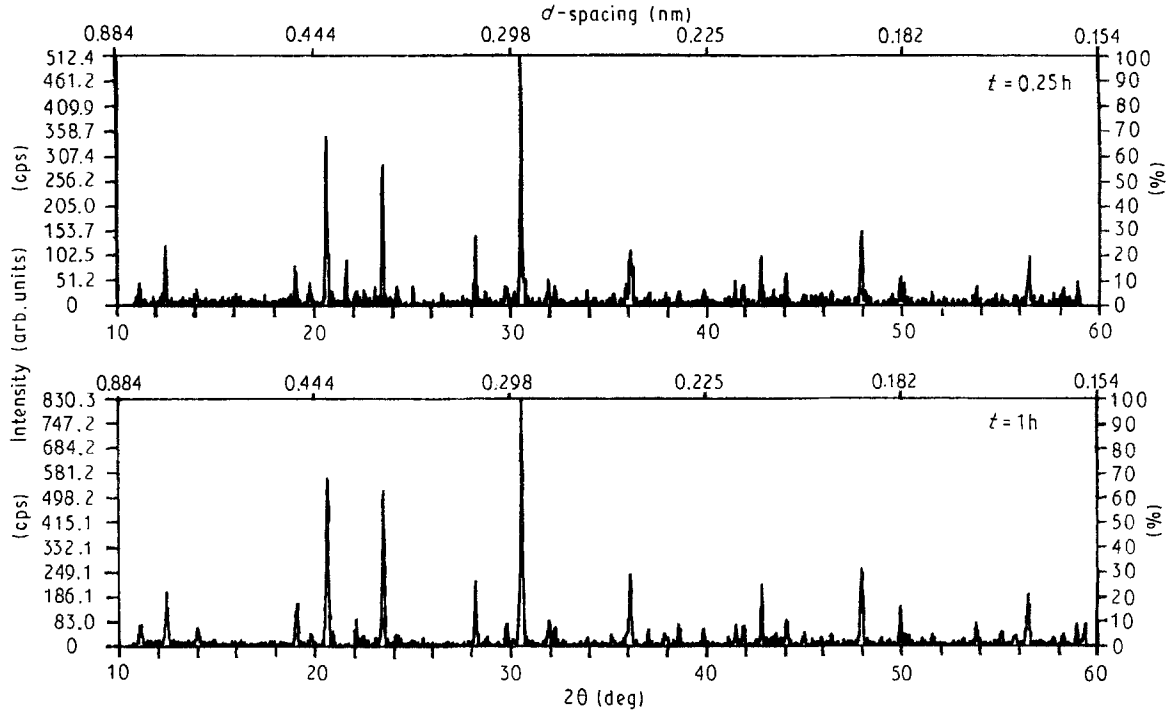

Figure 3 XRD patterns of BaZP samples sintered at 1600 °C, showing that the material sintered for 1 h is nearly single phase.

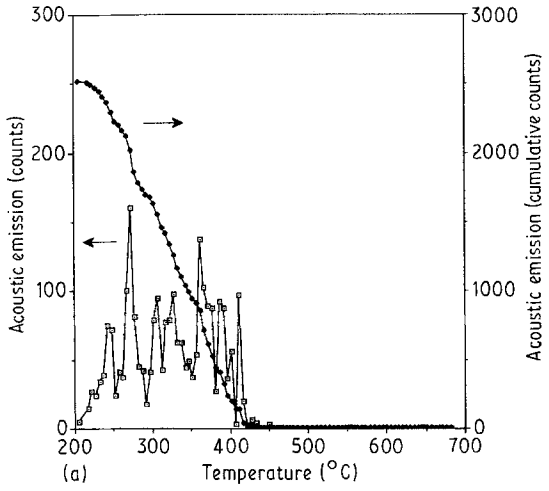

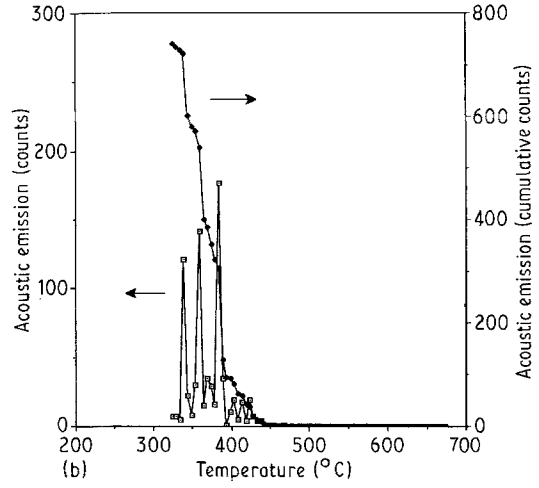

Figure 4 Acoustic emission data of BaZP samples sintered at (a) 1300 and (b) 1600 °C, showing total cumulative counts as well as counts at every 5 °C interval with temperature.

small amounts of secondary phases. It is inferred from the sintering results of BaZP that to obtain a single-phase material, one would need heat treatment at 1600 °C for at least 1 h, or at 1300 °C for more than 10 h.

3.3. Acoustic emission

Acoustic emission measurements were made on samples sintered at 1300 and 1600 °C only, as they contained nearly single-phase material of BaZP. The results are shown in Fig. 4 which includes the total number of counts, as well as counts recorded at every 5 °C interval when the samples were cooled from 700 °C to room temperature. In each case, no acoustic signals were detected during the heating cycle. All samples showed acoustic emission activity between

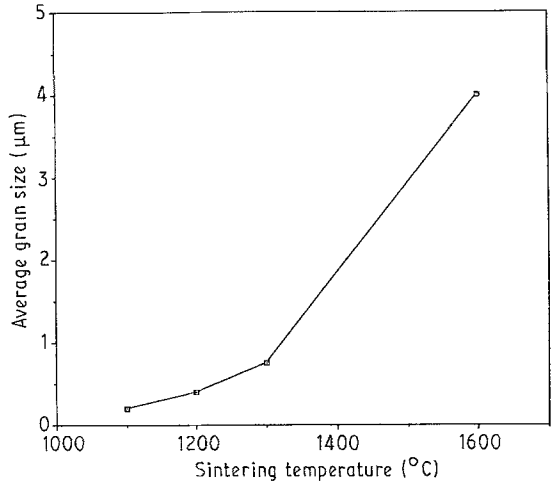

Figure 5 Average grain size of BaZP samples as a function of sintering temperature for 1 h sintering time.

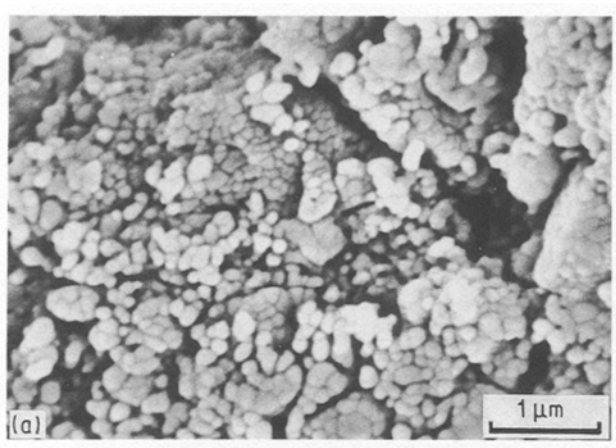

Figure 6 SEMs of BaZP samples sintered at 1100 °C for (a) 0.2, (b) 1.0 and (c) 10.0 h.

300 and 400 °C, indicating that this is the region in which microcracking most probably occurs. However, no definite pattern in the microcracking *vis-a-vis* sintering temperature or time could be observed. In each sample there were several large peaks which seemed to indicate microcracks forming in bursts. After the initial microcracks form, there was a period of relative inactivity until another burst of microcracks occurred. This may suggest that microcracks form and then propagate until enough internal stresses are developed to create another burst of microcracks. This hypothesis needs further verification.

3.4. Microstructure

Average grain size as estimated from the SEM micrographs of the sintered samples is plotted against the sintering temperature in Fig. 5, which shows that for 1 h sintering time the grains had grown from 0.2 μm at 1100 °C to about 4 μm at 1600 °C. Figs 6–9 show selected SEM micrographs of the samples sintered at various temperatures and times. The samples sintered at 1100 °C consist of large porosity as expected due to their low density (60% of theoretical), and an amorphous material located around the grain boundaries indicating an incomplete solid-state reaction. The grains were of submicrometre size, with rounded

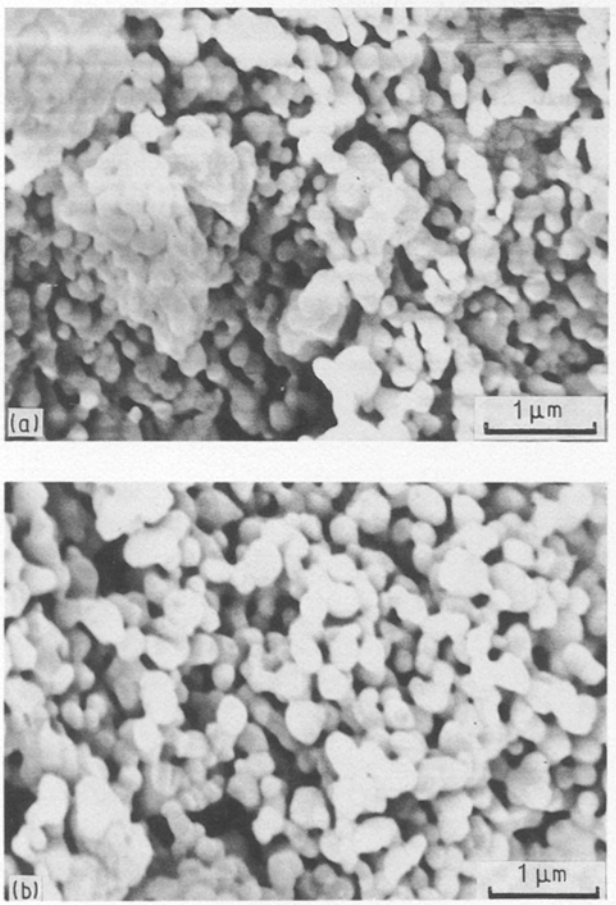

Figure 7 SEMs of BaZP samples sintered at 1200 °C for (a) 0.2, (b) 1.0 and (c) 10.0 h.

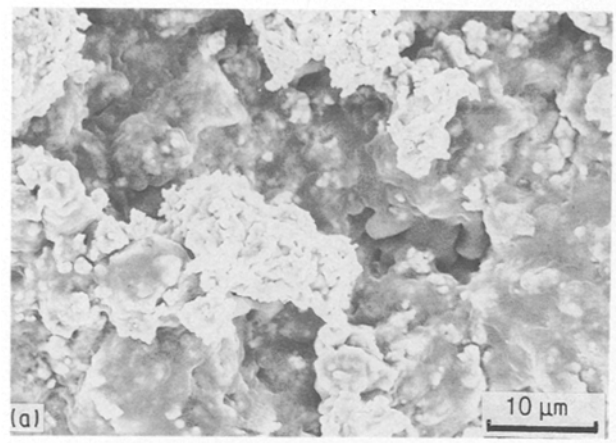

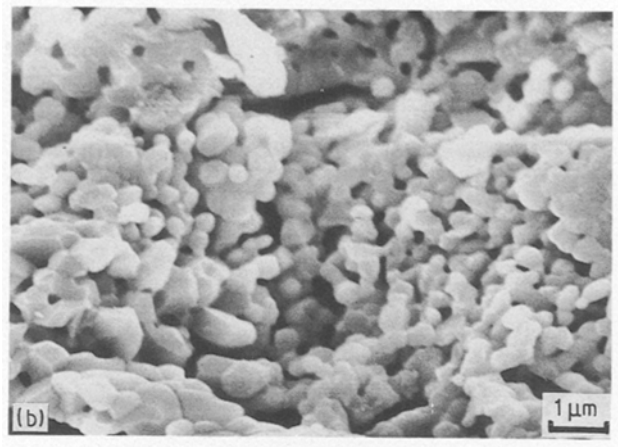

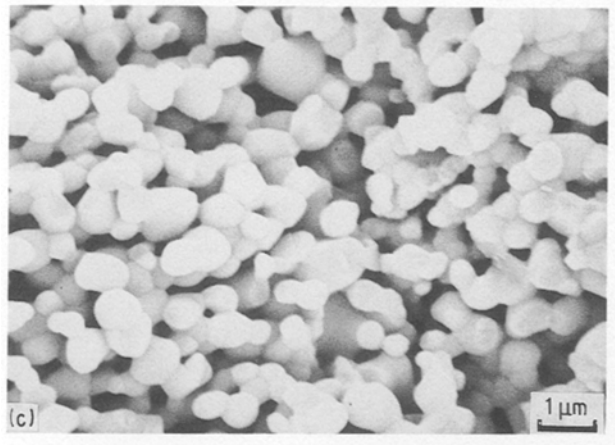

Figure 8 SEMs of BaZP samples sintered at 1300 °C for (a) 0.2, (b) 1.0 and (c) 10.0 h.

shape and poorly bonded, suggesting low mechanical strength, although there were areas of localized densification (Fig. 6c). The samples sintered at 1200 °C also have similar microstructure to that of the 1100 °C samples, except the grain size was little larger but still in the submicrometre range. The sample sintered for 10 h at 1200 °C (Fig. 7c) contained areas of high densification, although the overall microstructure was still very porous. A similar trend was also observed in the samples sintered at 1300 °C (Fig. 8), although the grains had grown to nearly 1 μm. The samples sintered at 1600 °C showed larger grains and relatively higher densification (Fig. 9). The grains appear to be strongly bonded, and there are fewer pores of both inter- and intra-granular nature. The typical grain size was between 2 and 5 μm. No amorphous phase in these specimens along the grain boundaries was observed, indicating the near completion of the reaction, as evidenced by the XRD patterns.

Apparently no microcracks, responsible for the acoustic emission activity, were observed by the SEM examination of the fractured surfaces of the sintered specimens of BaZP. This may be explained by the fact that the size and the number of microcracks are very small, and further the area usually examined under the SEM is in the range of 10–200 μm^2. Therefore it is highly unlikely that microcracks caused by thermal expansion anisotropy in the ceramics under study would show up under SEM.

4. Conclusion

The effects of various sintering parameters on the microstructure, phase composition and microcracking in $BaZr_4P_6O_{24}$ ceramics were investigated. It was found that single-phase material can be formed by heat treatment at 1600 °C for $\geqslant$ 1 h. The average grain size of the specimen sintered at 1600 °C was about 4 μm, though the samples sintered at lower temperatures consisted of grains of submicrometre size. The acoustic emission measurements made on the sintered

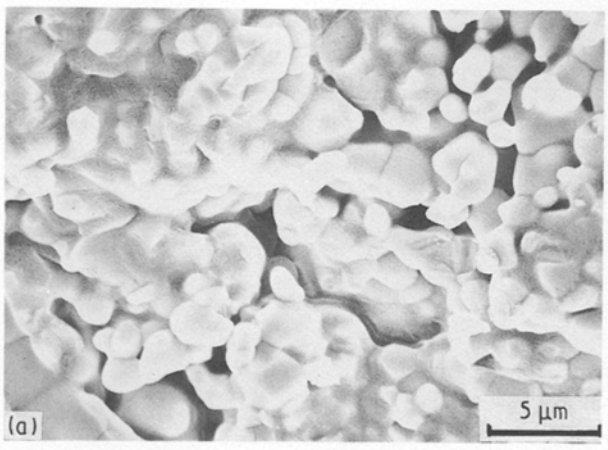

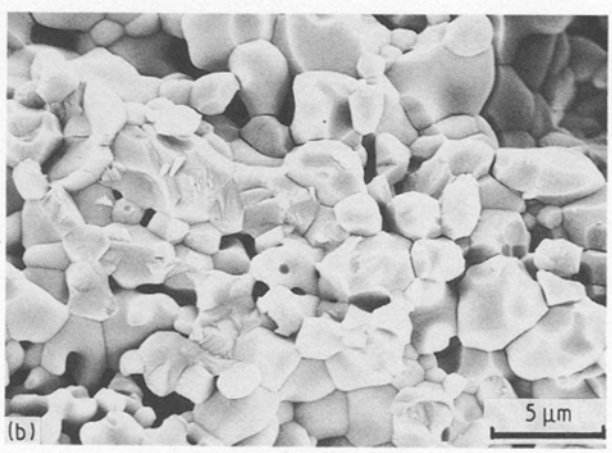

Figure 9 SEMs of BaZP samples sintered at 1600 °C for (a) 0.25 and (b) 1.0 h.

samples showed that during the cooling cycle, microcracks formed between 300 and 400 °C, and the change in sintering conditions did not substantially alter this activity.

References

1. J. ALAMO and R. ROY, *J. Amer. Ceram. Soc.* **67** (1984) C78.
2. R. ROY, D. K. AGRAWAL, J. ALAMO and R. A. ROY, *Mater. Res. Bull.* **19** (1984) 471.
3. J. B. GOODENOUGH, H. Y-P. HONG and J. A. KAFALAS, *ibid.* **11** (1976) 203.
4. R. ROY, D. K. AGRAWAL and H. A. McKINSTRY, *Ann. Rev. Mater. Sci.* **19** (1989) 59.
5. T. OOTA and I. YAMAI, *J. Amer. Ceram. Soc.* **69** (1986) 1.
6. T. OTA, P. JIN and I. YAMAI, *J. Mater. Sci.* **24** (1989) 4239.
7. R. ROY, E. R. VANCE and J. ALAMO, *Mater. Res. Bull.* **17** (1982) 585.
8. J. ALAMO and R. ROY, *J. Mater. Sci.* **21** (1986) 444.
9. L. O. HAGMAN and P. KIERKEGAARD, *Acta Chem. Scand.* **22** (1968) 1822.
10. G. E. LENAIN, H. A. McKINSTRY, J. ALAMO and D. K. AGRAWAL, *J. Mater. Sci.* **22** (1987) 17.
11. G. E. LENAIN, H. A. McKINSTRY, S. Y. LIMAYE and A. WOODWARD, *Mater. Res. Bull.* **19** (1984) 1451.
12. S. Y. LIMAYE, D. K. AGRAWAL and H. A. McKINSTRY, *J. Amer. Ceram. Soc.* **70** (1987) C232.
13. W. R. BUESSEM and F. F. LANGE, *Interceram.* **15** (1966) 229.
14. J. A. KUSYZK and R. C. BRADT, *J. Amer. Ceram. Soc.* **56** (1973) 420.
15. V. SRIKANTH, E. C. SUBBARAO, D. K. AGRAWAL, C.-Y. HUANG, R. ROY and G. V. RAO, *J. Amer. Ceram. Soc.* **74** (1991) 365.
16. K. LØNVIK, *Thermochim. Acta* **110** (1987) 253.
17. G. E. LENAIN, H. A. McKINSTRY and D. K. AGRAWAL, *J. Amer. Ceram. Soc.* **68** (1985) C224.

Received 8 January
and accepted 7 June 1991